Pergamon

Structural Engineering Review Vol. 6, No. 3–4, pp. 245–253, 1994

0952–5807/94 $7.00 + 0.00

0952–5807(94)E0024–U

THE USE OF MODIFIED BÉZIER TRIANGLES FOR THE FORM FINDING AND ANALYSIS OF CABLE NET STRUCTURES

C. J. K. Williams
School of Architecture and Building Engineering, University of Bath, Bath BA2 7AY, U.K.

(*Received* 16 *March* 1994; *accepted* 8 *April* 1994)

Abstract—A method is described for the form finding and analysis of cable net structures using curvilinear triangular finite elements. Each triangle is described by a complete cubic function of the two element coordinates plus two singular functions to give C^1 continuity.

The coefficients of the functions are controlled by 12 Bézier points, 10 for the cubic plus two extra points for the singular functions. There are five coordinates at each Bézier point, the three Cartesian coordinates and the 'cable number' for each of the two sets of cables making up the net.

INTRODUCTION

A typical cable net structure consists of two sets of steel cables with a spacing of 0.5 m between nodes where the cables cross and are clamped together. A cable net might span 100 m supported by masts and boundary cables, rather like a large tent.

Cable nets are prestressed by pulling on guy cables or by jacking up masts. The prestressing is required to give the structure stiffness to resist applied loads due to wind and snow. The net might be clad with a fabric, plastic panels, glass panels or even timber boarding and roof tiles.

The small squares formed by the crossing cables deform to diamond shapes as the net forms a surface of double curvature. This deformation would not be possible if the net consisted of three sets of crossing cables. The flexibility introduced by having only two sets of cables also allows the structure to deform to carry loads without "wrinkling".

The shape of a net in its prestressed state is determined by the elastic stiffness of the net and supporting structure and by the equations of static equilibrium. The process of finding the geometry of a net in its prestressed state is known as *form finding*. The shape of the net when flattened out is known as the *cutting pattern*.

The form-finding process typically consists of making rough models out of the stretchy material used for ladies' tights to represent the cable net and wooden dowels and cotton to represent the masts, boundary cables and guys. Once an acceptable rough form has been found, the structure is analysed numerically, making adjustments to the supports and to the cutting pattern until an acceptable form is found.

Once the form finding is complete, the structure is again analysed numerically to find the effect of wind and snow loads.

When the net structure is analysed numerically, both for the form finding and the analysis under load, it is invariably analysed as a system of straight line elements which can carry tension but not compression or twisting and bending moments. Limitations of computer storage and processing speed mean that each element has to represent a number of cables. Thus the cable grid of 0.5 m might be represented by a 5 m grid of elements in the computer model.

As the cutting pattern of the net is adjusted during the numerical form-finding process, elements have to be added and removed from the edge of the net. This makes the data preparation tedious and difficult to automate.

Ideally, there would be a finer grid of elements near boundaries and in areas of high curvature where greater accuracy is required. This is difficult to arrange if the computer model consists entirely of line elements.

This paper presents an alternative approach. The fine grid of a cable net relative to overall dimensions and radii of curvature means that the net can be approximated by a continuous curved surface. A surface can be represented numerically using finite elements or the surface patches used in computer-aided geometric design (which are essentially the same thing).

The net of cables can be thought of as forming two sets of coordinate curves on each element. The position of a point on the surface can be described by the 'cable number' of each of the two cables crossing at the point. A cable is a contour of constant cable number, just like one might have contours of constant temperature.

The elements described in this paper are curvilinear triangles and the net of cables form curvilinear lines on the elements. One could use curvilinear elements of any shape; many surface patches are curvilinear quadrilaterals. The advantage of

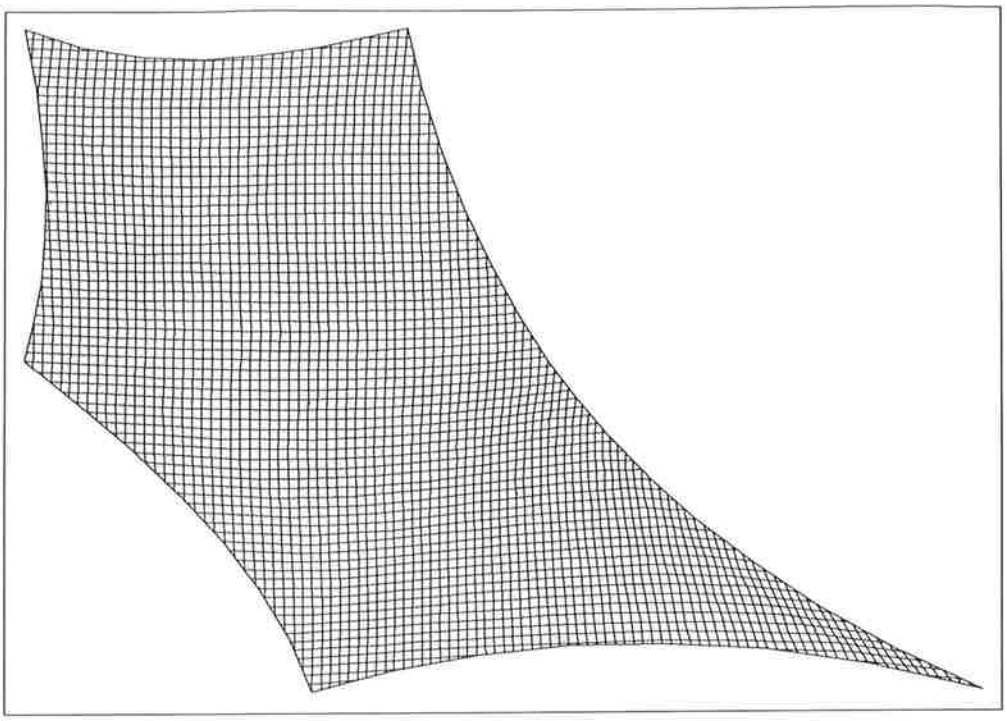

Fig. 1. Plan of prestressed cable net.

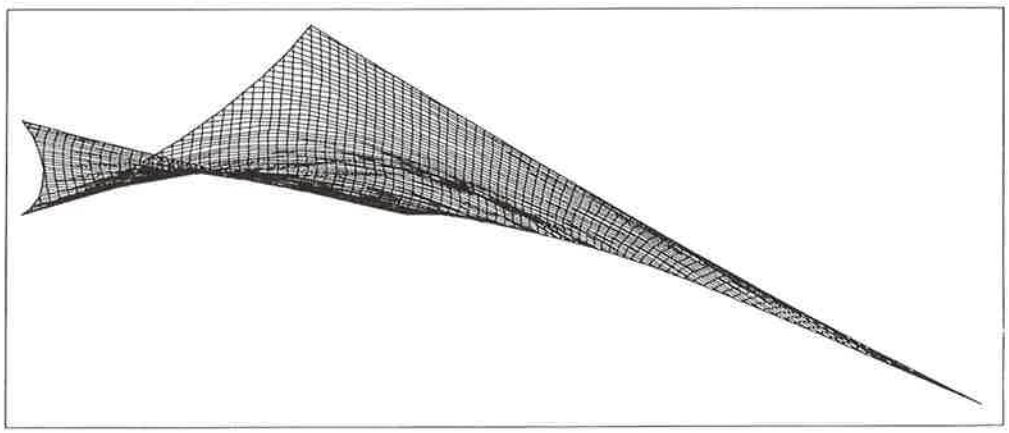

Fig. 2. Elevation of prestressed cable net.

triangles is that they easily allow extra elements to be introduced in areas where greater accuracy is required.

It would also be possible to use flat triangular elements to represent the curved surface by a faceted surface. This would be simpler, but would require a larger number of elements and degrees of freedom to achieve the same level of accuracy.

The formulation used in this paper achieves C^1 continuity which means that the tangents to the surface elements and to the cables on the element are continuous across the boundary between adjacent elements. Thus there are no 'kinks' in the cables where they cross from one element to the next.

Figures 1–5 show what can be achieved with this approach. Figures 1, 2 and 3 show a plan and two elevations of a cable net in its prestressed state. Figure 4 shows the cutting pattern and Fig. 5 is a repeat of Fig. 1 with the cables removed, but with the addition of the boundaries of the four curvilinear triangles forming the surface. Note that the figures are not all drawn to the same scale.

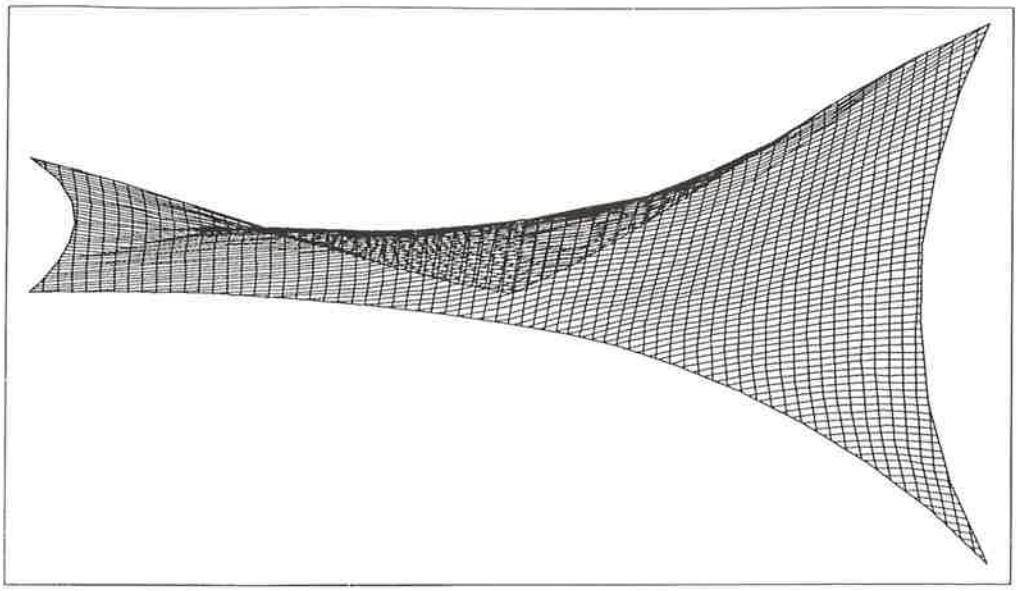

Fig. 3. Elevation of prestressed cable net.

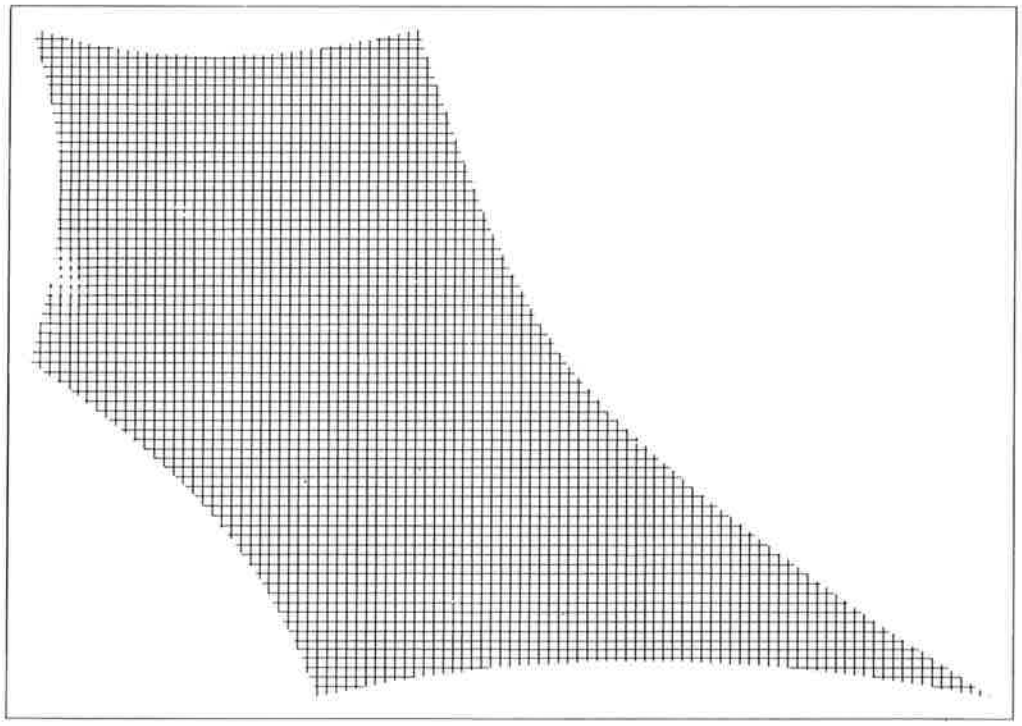

Fig. 4. Cutting pattern of cable net.

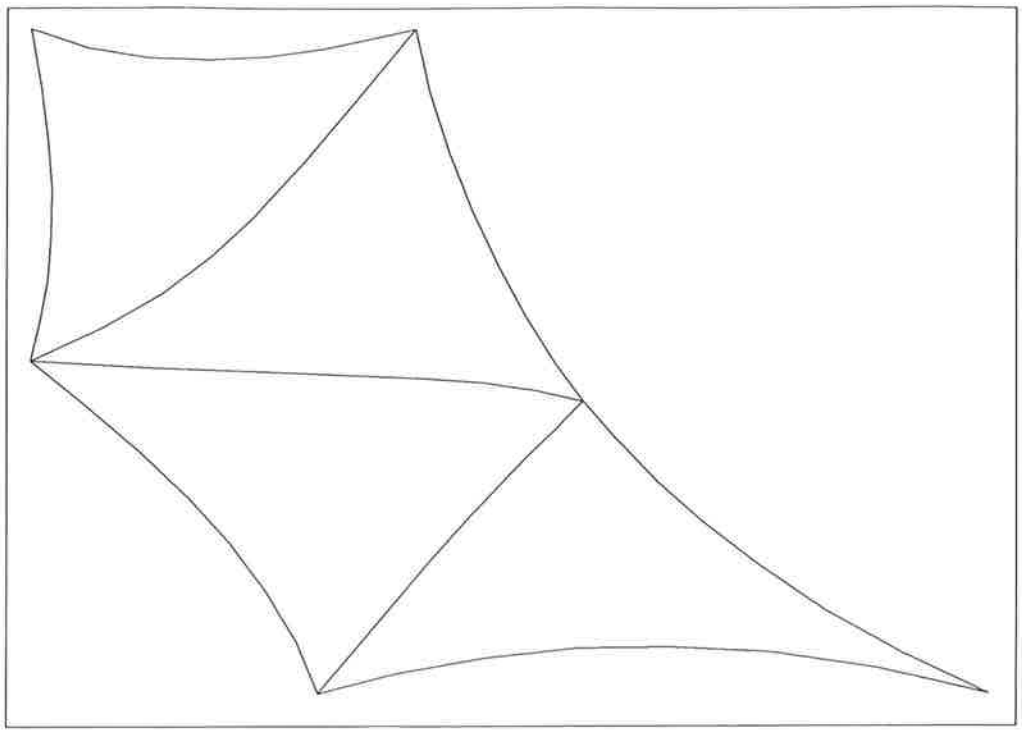

Fig. 5. Curvilinear triangles forming the surface shown in Figs 1–3.

ELEMENT FORMULATION

The shape of a single triangular element is defined by the three functions

$$\left.\begin{aligned} x &= x(u, v), \\ y &= y(u, v) \\ \text{and } z &= z(u, v), \end{aligned}\right\} \tag{1}$$

where x, y and z are Cartesian coordinates and u and v are parameters or surface coordinates. Each triangle will have different coefficients in the functions (1) and the aim is to choose the coefficients in such a way as to provide a given degree of continuity between adjacent triangles.

The edges of a triangle are defined by

$$\left.\begin{aligned} u &= 0, \\ v &= 0 \\ \text{and } u + v &= 1. \end{aligned}\right\} \tag{2}$$

In order to simplify the form of the functions (1) we will introduce the variable

$$w = 1 - u - v, \tag{3}$$

so that

$$w = 0 \tag{4}$$

on the side on which $u + v = 1$.

The layout of the cable net on the triangle is defined by the functions

$$\left.\begin{aligned} \theta &= \theta(u, v) \\ \text{and } \phi &= \phi(u, v) \end{aligned}\right\} \tag{5}$$

and along an individual cable

$$\left.\begin{aligned} \theta &= \text{constant} \\ \text{or } \phi &= \text{constant}. \end{aligned}\right\} \tag{6}$$

The two functions (5) give the relationship between the two sets of surface coordinates, (θ, ϕ) and (u, v). The three functions (1) and the two functions (5) will be based on the Bézier triangles described in Farin.[1] If x, y, z, θ and ϕ are elements of the column matrix or vector,

$$\mathbf{p} = \begin{bmatrix} x \\ y \\ z \\ \theta \\ \phi \end{bmatrix}, \tag{7}$$

then the cubic Bézier triangle formulation gives

$$\begin{aligned} \mathbf{p} = {} & \mathbf{b}_{030} B^3_{030} \\ & + \mathbf{b}_{021} B^3_{021} + \mathbf{b}_{120} B^3_{120} \\ & + \mathbf{b}_{012} B^3_{012} + \mathbf{b}_{111} B^3_{111} + \mathbf{b}_{210} B^3_{210} \\ & + \mathbf{b}_{003} B^3_{003} + \mathbf{b}_{102} B^3_{102} + \mathbf{b}_{201} B^3_{201} + \mathbf{b}_{300} B^3_{300}, \end{aligned} \tag{8}$$

in which $\mathbf{b}_{ijk}$ are column matrices, each containing 5 d.f. corresponding to the x to ϕ in Eq. (7). B^n_{ijk} are the Bernstein polynomials,

$$B^n_{ijk} = \frac{n!}{i!\,j!\,k!} u^i v^j w^k. \tag{9}$$

It can be demonstrated that Eq. (8) contains all the 10 terms of a complete cubic polynomial in u and v.

We shall refer to the "point" $\mathbf{p}$ with coordinates x to ϕ and we shall describe the $\mathbf{b}_{ijk}$ as control points. The physical meaning of some of the $\mathbf{b}_{ijk}$ can be seen by observing that

$$\left.\begin{aligned} &\text{when } u = 1,\ v = 0 \quad (\text{and } w = 0),\ \mathbf{p} = \mathbf{b}_{300},\\ &\text{when } u = 0,\ v = 1 \quad (\text{and } w = 0),\ \mathbf{p} = \mathbf{b}_{030}\\ &\text{and when } u = v = 0 \quad (\text{and } w = 1),\ \mathbf{p} = \mathbf{b}_{003}. \end{aligned}\right\} \tag{10}$$

Thus $\mathbf{b}_{300}$, $\mathbf{b}_{030}$ and $\mathbf{b}_{003}$ are the points at the corners of the triangle and this partly explains why the right-hand side of Eq. (8) is written in triangular form. However, in general, the remainder of the points $\mathbf{b}_{ijk}$ do not lie on the surface of the triangle.

We shall now introduce a modification in which the term $\mathbf{b}_{111}B^3_{111}$ is replaced by $\mathbf{b}_{\{1\}11}B^3_{\{1\}11} + \mathbf{b}_{11\{1\}}B^3_{11\{1\}} + \mathbf{b}_{1\{1\}1}B^3_{1\{1\}1}$ to give

$$\begin{aligned} \mathbf{p} = {} & \mathbf{b}_{030}B^3_{030} \\ & + \mathbf{b}_{021}B^3_{021} + \mathbf{b}_{120}B^3_{120} \\ & + \mathbf{b}_{\{1\}11}B^3_{\{1\}11} + \mathbf{b}_{11\{1\}}B^3_{11\{1\}} \\ & + \mathbf{b}_{012}B^3_{012} \qquad\qquad + \mathbf{b}_{210}B^3_{210} \\ & + \mathbf{b}_{1\{1\}1}B^3_{1\{1\}1} \\ & + \mathbf{b}_{003}B^3_{003} + \mathbf{b}_{102}B^3_{102} + \mathbf{b}_{201}B^3_{201} + \mathbf{b}_{300}B^3_{300}. \end{aligned} \tag{11}$$

The control points $\mathbf{b}_{\{1\}11}$, $\mathbf{b}_{11\{1\}}$ and $\mathbf{b}_{1\{1\}1}$ can again be written as column matrices, each containing 5 d.f. The functions

$$\left.\begin{aligned} B^3_{\{1\}11} &= \frac{6uvw}{(u+v)(v+w)(w+u)} vw\left(1-\frac{u}{3}\right),\\ B^3_{1\{1\}1} &= \frac{6uvw}{(u+v)(v+w)(w+u)} wu\left(1-\frac{v}{3}\right)\\ \text{and } B^3_{11\{1\}} &= \frac{6uvw}{(u+v)(v+w)(w+u)} uv\left(1-\frac{w}{3}\right). \end{aligned}\right\} \tag{12}$$

Using Eq. (3), it is easy to demonstrate that

$$B^3_{\{1\}11} + B^3_{1\{1\}1} + B^3_{11\{1\}} = B^3_{111} \tag{13}$$

and therefore Eq. (11) is equivalent to the complete cubic polynomial (8) plus two extra functions.

The functions (12) are singular in that they tend to infinity as

$(u+v)\to 0$ unless u and v simultaneously $\to 0$,

$(v+w)\to 0$ unless v and w simultaneously $\to 0$

or $(w+u)\to 0$ unless w and u simultaneously $\to 0$.

It can be demonstrated that the functions (12) remain finite within the boundaries of the triangle given by (2) and (4) and that they remain finite on the edges and at the corners of the triangle. It can also be demonstrated that the first and second partial derivatives of the functions (12) with respect to u and/or v remain finite within, on the edges or at the corners of the triangle. In forming the partial derivatives, it follows from Eq. (3) that

$$\left.\begin{aligned} \frac{\partial w}{\partial u} &= -1\\ \text{and } \frac{\partial w}{\partial v} &= -1. \end{aligned}\right\} \tag{14}$$

Singular functions, similar but not identical to Eq. (12), are given in Zienkiewicz.[2]

BASE VECTORS

The position vector of typical point on a triangle can be written

$$\mathbf{r} = \begin{bmatrix} x \\ y \\ z \end{bmatrix} \tag{15}$$

and clearly $\mathbf{r}$ can be obtained from $\mathbf{p}$ which in turn is obtained from Eq. (11). The two base vectors,

$$\left.\begin{aligned} \mathbf{r}_{,\theta} &= \frac{\partial \mathbf{r}}{\partial \theta}\\ \text{and } \mathbf{r}_{,\phi} &= \frac{\partial \mathbf{r}}{\partial \phi} \end{aligned}\right\} \tag{16}$$

(where the comma denotes partial differentiation) are both tangent to the surface of a triangle. $\mathbf{r}_{,\theta}$ is tangent to a cable ϕ = constant and $\mathbf{r}_{,\phi}$ is tangent to a cable θ = constant.

Solving the equations

$$\left.\begin{aligned} \delta\theta &= \theta_{,u}\delta u + \theta_{,v}\delta v\\ \text{and } \delta\phi &= \phi_{,u}\delta u + \phi_{,v}\delta v \end{aligned}\right\} \tag{17}$$

(where again the comma denotes partial differentiation) gives

$$\left.\begin{aligned} u_{,\theta} &= \frac{\phi_{,v}}{\theta_{,u}\phi_{,v} - \phi_{,u}\theta_{,v}}, \\ u_{,\phi} &= \frac{-\theta_{,v}}{\theta_{,u}\phi_{,v} - \phi_{,u}\theta_{,v}}, \\ v_{,\theta} &= \frac{-\phi_{,u}}{\theta_{,u}\phi_{,v} - \phi_{,u}\theta_{,v}} \\ \text{and } v_{,\phi} &= \frac{\theta_{,u}}{\theta_{,u}\phi_{,v} - \phi_{,u}\theta_{,v}}. \end{aligned}\right\} \tag{18}$$

Hence

$$\left.\begin{aligned} \mathbf{r}_{,\theta} &= \frac{\mathbf{r}_{,u}\phi_{,v} - \phi_{,u}\mathbf{r}_{,v}}{\theta_{,u}\phi_{,v} - \phi_{,u}\theta_{,v}} \\ \text{and } \mathbf{r}_{,\phi} &= \frac{\theta_{,u}\mathbf{r}_{,v} - \mathbf{r}_{,u}\theta_{,v}}{\theta_{,u}\phi_{,v} - \phi_{,u}\theta_{,v}}. \end{aligned}\right\} \tag{19}$$

The right-hand sides of Eqs (18) and (19) can be obtained by partially differentiating Eq. (11) with respect to u or v and making use of Eq. (14).

CONTINUITY BETWEEN ADJACENT ELEMENTS

Along the edge $v = 0$ of a triangle we have $w = 1 - u$ and, from Eqs (11), (9) and (12),

$$\mathbf{p} = (1-u)^3\mathbf{b}_{003} + 3u(1-u)^2\mathbf{b}_{102} + 3u^2(1-u)\mathbf{b}_{201} + u^3\mathbf{b}_{300}. \tag{20}$$

Thus, if two adjacent triangles share the same four control points along their common boundary, there is automatic continuity in x, y, z, θ and ϕ.

If we differentiate Eq. (11) partially with respect to u using Eq. (14) and then set $v = 0$, we obtain

$$\mathbf{p}_{,u} = 3(1-u)^2(\mathbf{b}_{102} - \mathbf{b}_{003}) + 6u(1-u)(\mathbf{b}_{201} - \mathbf{b}_{102}) + 3u^2(\mathbf{b}_{300} - \mathbf{b}_{201}) \tag{21}$$

and if we differentiate Eq. (11) partially with respect to v [again using Eq. (14)] and then set $v = 0$ we obtain

$$\mathbf{p}_{,v} = 3(1-u)^2(\mathbf{b}_{012} - \mathbf{b}_{003}) + 6u(1-u)(\mathbf{b}_{1\{1\}1} - \mathbf{b}_{102}) + 3u^2(\mathbf{b}_{210} - \mathbf{b}_{201}). \tag{22}$$

We shall now see how continuity of $\mathbf{r}_{,\theta}$ and $\mathbf{r}_{,\phi}$ can be obtained across the boundary between two adjacent triangular elements. For simplicity we shall assume that the two triangles meet along the edges $v = 0$ of each triangle. There is no reason why this should be so and it is easy to extend the argument to the general case. We shall also assume that the triangles are orientated so that two corners $u = 0$ touch each other and again this is not a necessary requirement.

Let us write the control points of the two triangles as $\mathbf{b}_{003}, \mathbf{b}_{102}, \ldots \mathbf{b}_{1\{1\}1}, \ldots$ and $\bar{\mathbf{b}}_{003}, \bar{\mathbf{b}}_{102}, \ldots \bar{\mathbf{b}}_{1\{1\}1}, \ldots$. The vectors containing coordinates will be written as $\mathbf{p}$ and $\bar{\mathbf{p}}$. We have already discussed the requirement for continuity of position across the boundary (i.e. $\mathbf{p} = \bar{\mathbf{p}}$) which is

$$\left.\begin{aligned} \bar{\mathbf{b}}_{003} &= \mathbf{b}_{003}, \\ \bar{\mathbf{b}}_{102} &= \mathbf{b}_{102}, \\ \bar{\mathbf{b}}_{201} &= \mathbf{b}_{201} \\ \text{and } \bar{\mathbf{b}}_{300} &= \mathbf{b}_{300}. \end{aligned}\right\} \tag{23}$$

We shall now demonstrate that there will be continuity of $\mathbf{r}_{,\theta}$ and $\mathbf{r}_{,\phi}$ if

$$\left.\begin{aligned} &\bar{\mathbf{b}}_{012} - \bar{\mathbf{b}}_{003} = \lambda(\mathbf{b}_{102} - \mathbf{b}_{003}) + \mu(\mathbf{b}_{012} - \mathbf{b}_{003}), \\ &\bar{\mathbf{b}}_{1\{1\}1} - \bar{\mathbf{b}}_{102} = \lambda(\mathbf{b}_{201} - \mathbf{b}_{102}) + \mu(\mathbf{b}_{1\{1\}1} - \mathbf{b}_{102}) \\ &\text{and} \\ &\bar{\mathbf{b}}_{210} - \bar{\mathbf{b}}_{201} = \lambda(\mathbf{b}_{300} - \mathbf{b}_{201}) + \mu(\mathbf{b}_{210} - \mathbf{b}_{201}), \end{aligned}\right\} \tag{24}$$

where λ and μ are constants for this particular boundary between two triangles, but may have different values on other boundaries. It follows from Eqs (21)–(24) that

$$\left.\begin{aligned} \bar{\mathbf{p}}_{,u} &= \mathbf{p}_{,u} \\ \text{and } \bar{\mathbf{p}}_{,v} &= \lambda\mathbf{p}_{,u} + \mu\mathbf{p}_{,v}, \end{aligned}\right\} \tag{25}$$

Now substituting Eq. (25) into the first equation (19) gives

$$\bar{\mathbf{r}}_{,\theta} = \frac{\mathbf{r}_{,u}(\lambda\phi_{,u} + \nu\phi_{,v}) - \phi_{,u}(\lambda\mathbf{r}_{,u} + \mu\mathbf{r}_{,v})}{\theta_{,u}(\lambda\phi_{,u} + \mu\phi_{,v}) - \phi_{,u}(\lambda\theta_{,u} + \mu\theta_{,v})} = \frac{\mathbf{r}_{,u}\phi_{,v} - \phi_{,u}\mathbf{r}_{,v}}{\theta_{,u}\phi_{,v} - \phi_{,u}\theta_{,v}} = \mathbf{r}_{,\theta} \tag{26}$$

and similarly

$$\bar{\mathbf{r}}_{,\phi} = \mathbf{r}_{,\phi}. \tag{27}$$

Thus conditions (23) and (24) ensure that cables cross from one element to another with a continuous tangent.

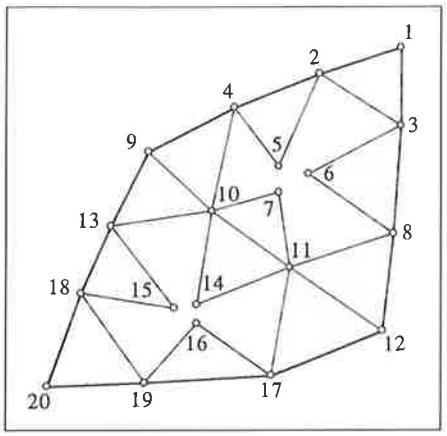

Fig. 6. Control points for two adjacent curvilinear triangles.

Figure 6 shows the control points for two adjacent curvilinear triangular elements. The elements themselves are not shown and remember that, in general, an element only passes through its three corner control points. In Fig. 6 each node is given only one number instead of the three used to denote each of $\mathbf{b}_{003}$, $\mathbf{b}_{102}$, . . . $\mathbf{b}_{1\{1\}1}$, . . . and $\bar{\mathbf{b}}_{003}$, $\bar{\mathbf{b}}_{102}$, . . . $\bar{\mathbf{b}}_{1\{1\}1}$, ... If we use square brackets to denote this single number notation, then for the triangle on the upper right of Fig. 6,

$$\left.\begin{aligned} \mathbf{b}_{030} &= \mathbf{b}_{[1]}, \\ &\vdots \\ \mathbf{b}_{1\{1\}1} &= \mathbf{b}_{[7]}, \\ &\vdots \\ \mathbf{b}_{102} &= \mathbf{b}_{[10]}, \\ &\vdots \end{aligned}\right\} \tag{28}$$

which corresponds to the layout of Eq. (11). For the triangle on the lower left of Fig. 6,

$$\left.\begin{aligned} \bar{\mathbf{b}}_{030} &= \mathbf{b}_{[20]}, \\ &\vdots \\ \bar{\mathbf{b}}_{1\{1\}1} &= \mathbf{b}_{[14]}, \\ &\vdots \\ \bar{\mathbf{b}}_{102} &= \mathbf{b}_{[10]}, \\ &\vdots \end{aligned}\right\} \tag{29}$$

The two triangles share the four points $\mathbf{b}_{[9]}$, $\mathbf{b}_{[10]}$, $\mathbf{b}_{[11]}$ and $\mathbf{b}_{[12]}$ and this ensures continuity of position between the two elements. The conditions for continuity of the tangents to the net cables, Eq. (24), become

$$\left.\begin{aligned} \mathbf{b}_{[13]} - \mathbf{b}_{[9]} &= \lambda(\mathbf{b}_{[10]} - \mathbf{b}_{[9]}) + \mu(\mathbf{b}_{[4]} - \mathbf{b}_{[9]}), \\ \mathbf{b}_{[14]} - \mathbf{b}_{[10]} &= \lambda(\mathbf{b}_{[11]} - \mathbf{b}_{[10]}) - \mu(\mathbf{b}_{[7]} - \mathbf{b}_{[10]}) \\ \text{and} & \\ \mathbf{b}_{[17]} - \mathbf{b}_{[11]} &= \lambda(\mathbf{b}_{[12]} - \mathbf{b}_{[11]}) + \mu(\mathbf{b}_{[8]} - \mathbf{b}_{[11]}). \end{aligned}\right\} \tag{30}$$

The symmetry of the formulation of the triangles means that conditions (30) will continue to ensure continuity of position and tangents if the sides $u = 0$, $v = 0$ and $w = 0$ are changed on one or both of the triangles.

The conditions (30) can be expressed geometrically and Fig. 7 shows how this was done in preparing the data which eventually led to Figs 1–5. In Fig. 7, each triangular element is drawn with straight sides even though the element will eventually be curved. All angles on Fig. 7 are 45 or 90°, although this does not have to be the case.

Each triangle is divided up by joining the third points of each side with straight lines. The three central nodes of each triangle are coincident even though they are separated on the figure. The x, y, z, θ and ϕ coordinates of the control points corresponding to the nodes shown in black are determined by the x, y, z, θ and ϕ coordinates of the control points corresponding to the nodes shown in white. This is done by weighting the coordinates in proportion to the geometry of the figure. Thus, for example,

$$\begin{aligned} \mathbf{b}_{[30]} &= \frac{\mathbf{b}_{[27]} + \mathbf{b}_{[2]}}{2} + \left(\frac{\mathbf{b}_{[27]} + \mathbf{b}_{[2]}}{2} - \mathbf{b}_{[1]} \right) \\ &= \mathbf{b}_{[27]} + \mathbf{b}_{[2]} - \mathbf{b}_{[1]} \end{aligned} \tag{31}$$

and

$$\begin{aligned} \mathbf{b}_{[33]} &= \frac{\mathbf{b}_{[27]} + \mathbf{b}_{[30]}}{2} + \left(\frac{\mathbf{b}_{[27]} + \mathbf{b}_{[30]}}{2} - \frac{\mathbf{b}_{[27]} + \mathbf{b}_{[2]}}{2} \right) \\ &= \mathbf{b}_{[30]} + \frac{\mathbf{b}_{[27]} - \mathbf{b}_{[2]}}{2} = \frac{\mathbf{b}_{[27]} + \mathbf{b}_{[2]} - 2\mathbf{b}_{[1]}}{2}. \end{aligned} \tag{32}$$

It is, perhaps, now apparent why the singular functions were introduced into Eq. (11). The singular functions mean that there are now three control points away from the edges of each triangle, whereas the usual Bézier cubic has only one central point. Without the extra two points it is difficult to satisfy the conditions for continuity of tangents when there is a large number of triangles.

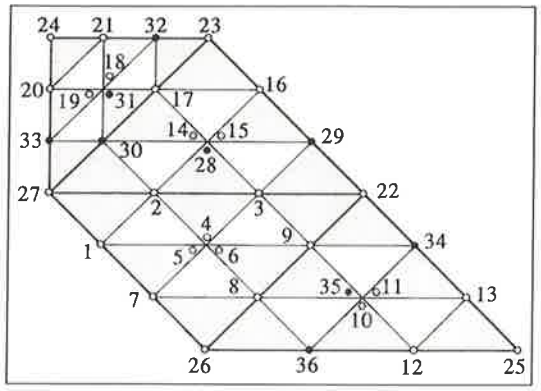

Fig. 7. Control points used to produce Figs 1–5.

MINIMISATION OF TOTAL POTENTIAL ENERGY

A real cable net will automatically find a shape in which the tensions in the cables are in static equilibrium with any applied loads—we shall only consider the static case, not a moving net. Alternatively, one can say that the net automatically finds a shape which minimises the total potential energy of the system. The total potential energy is the elastic strain energy of the net and its supporting structure plus the potential energy of any applied loads. The energy approach is to be preferred in the finite element method since it leads to integrals which have to be minimised.

In order to derive an expression for the strain energy of a cable net, let us first consider a single cable of length L under tension T. The slack length of the cable is L_0 and its stiffness is EA (where E is Young's modulus and A is the cross-sectional area, although for a real cable either E or A may have to be adjusted to take into account extra flexibility due to effects such as the twisting of the wires which make up the cable). The tension in the cable,

$$T = EA\frac{(L-L_0)}{L_0} \tag{33}$$

and the elastic strain energy stored in the cable is

$$\tfrac{1}{2}T(L-L_0) = EA\frac{(L-L_0)^2}{2L_0}. \tag{34}$$

Lengths are calculated using scalar products (or Pythagoras' theorem which amounts to the same thing). To avoid taking square roots in the computation, one can make use of the fact the L and L_0 are almost equal for most real cables to make the approximation

$$EA\frac{(L-L_0)^2}{2L_0} \approx EA\frac{(L+L_0)^2(L-L_0)^2}{8L_0^3} = EA\frac{(L^2-L_0^2)^2}{8L_0^3}. \tag{35}$$

Cables can only carry tension, not compression, and therefore the expression (35) should be set equal to zero if $L < L_0$.

If we adopt the notation

$$a_{\theta\theta} = \mathbf{r}_{,\theta}\cdot\mathbf{r}_{,\theta} \quad \text{and} \quad a_{\phi\phi} = \mathbf{r}_{,\phi}\cdot\mathbf{r}_{,\phi}, \tag{36}$$

then the strain energy of an element of cable on which ϕ is constant is equal to

$$(EA)_{\theta\theta}\frac{(a_{\theta\theta}-a_{\theta\theta_0})^2}{8(a_{\theta\theta_0})^{3/2}}\,\mathrm{d}\theta, \tag{37}$$

where $a_{\theta\theta_0}$ is the value of $a_{\theta\theta}$ when the cable is unstrained, $(EA)_{\theta\theta}$ is the axial stiffness of the cable and $\mathrm{d}\theta$ is the length of the cable in θ–ϕ space. If the cables on which ϕ is constant are at intervals $\Delta\phi$, then

$$\frac{(EA)_{\theta\theta}(a_{\theta\theta}-a_{\theta\theta_0})^2}{8\Delta\phi(a_{\theta\theta_0})^{3/2}}\,\mathrm{d}\theta\,\mathrm{d}\phi \tag{38}$$

is the strain energy of this set of cables in an area corresponding to $\mathrm{d}\theta\,\mathrm{d}\phi$ in θ–ϕ space.

Thus, including the second set of cables, the total strain energy of the cable net,

$$U_{\text{net}} = \int\int\left(\frac{(EA)_{\theta\theta}(a_{\theta\theta}-a_{\theta\theta_0})^2}{8\Delta\phi(a_{\theta\theta_0})^{3/2}} + \frac{(EA)_{\phi\phi}(a_{\phi\phi}-a_{\phi\phi_0})^2}{8\Delta\theta(a_{\phi\phi_0})^{3/2}}\right)(\theta_{,u}\phi_{,v}-\phi_{,u}\theta_{,v})\,\mathrm{d}u\,\mathrm{d}v, \tag{39}$$

in which the integration extends over all the triangular elements representing the net.

The strain energy of boundary cables, masts and other supporting structure and the potential energy of any loads can be calculated using the usual methods of structural analysis.

NUMERICAL IMPLEMENTATION

The geometry and total potential energy of a net structure is determined by the values of the x, y, z, θ and ϕ coordinates of the control points $\mathbf{b}_{[1]}$, $\mathbf{b}_{[2]}$ . . . as well as the physical properties of the net and the values of any loads. We now have to minimise the total potential energy subject to certain constraints.

In the form-finding process which led to Figs 1–5, only the x, y and z coordinates of control points 1–22 in Fig. 7 were allowed to change in the minimisation process. The x, y and z coordinates of

control points 23–27 remained fixed which corresponds to these points being fixed to rigid supports—they could equally well have been fixed to guyed masts. The coordinates of control points 28–36 are determined by the coordinates of control points 1–27 to maintain continuity of tangents as described earlier.

The boundary cables were taken as having a constant tension so that their strain energies are just proportional to their lengths. If one were to perform a subsequent structural analysis to find the effect of applied loads, then the boundary cables would be given appropriate stiffnesses and slack lengths to give the correct tension in the prestress condition.

The fact that the values of θ and ϕ at the control points do not change during the form finding means that the cutting pattern remains the same. However, one could imagine situations where one wants the cutting pattern to adjust itself automatically during the form finding.

Let us call the quantities which are allowed to vary the degrees of freedom and use the symbols $\delta_1 \ldots \delta_i \ldots \delta_N$. In the case of our example $N = 3 \times 23$. To minimise the total potential energy we require that

$$\frac{\partial U}{\partial \delta_1} = \ldots \frac{\partial U}{\partial \delta_i} = \ldots \frac{\partial U}{\partial \delta_N} = 0, \tag{40}$$

where U is the total potential energy.

The iterative algorithm used to find δ_i to satisfy Eq. (40) was based on the Dynamic Relaxation method first proposed by Alister Day[3] which can be written

$$(\delta_i)_{n+1} = (\delta_i)_n - \xi \left(\frac{\dfrac{\partial U}{\partial \delta_i}}{\dfrac{\partial^2 U}{\partial \delta_i^2}} \right)_n + \zeta \{(\delta_i)_n - (\delta_i)_{n-1}\}, \tag{41}$$

where n refers to the cycle number and ξ and ζ (<1.0) are dimensionless constants chosen by trial and error to obtain the fastest convergence.

The quantities $\partial U/\partial \delta_i$ and $\partial^2 U/\partial \delta_i^2$ were obtained by numerical integration using a regular array of 21 points for each triangle. The geometry shown in Figs 1–3 was obtained after 50 cycles when $\partial U/\partial \delta_i$ were considered to be sufficiently small. The arbitrary starting geometry was a flat net with only the support points moved out of the plane.

An over-relaxation factor, ξ, of 1.5 was used together with $\zeta = 0.7$. It was also found necessary to specify a minimum value for the "stiffnesses", $\partial^2 U/\partial \delta_i^2$, since very low or zero stiffnesses can occur during the analysis.

The form finding took approximately 2 h to run on a Macintosh Plus computer. Most of the time was spent performing the numerical integrations. The program was also run on a mainframe when it took a few seconds to perform the same 50 cycles.

Figures 1–5 were also produced on the Macintosh Plus. Each figure took about 2 min to calculate. The cable nets were drawn on the elements by constructing contour lines of constant θ and ϕ and this was done by dividing each element into a number of smaller triangles in which x, y, z, θ and ϕ were taken as linear functions of u and v. These small flat triangular facets can be seen upon close examination of Fig. 2.

OTHER POSSIBLE USES OF MODIFIED BÉZIER TRIANGLES

This paper has described the use of modified Bézier triangles for the analysis of cable nets. However, the ease with which continuity of tangents can be achieved suggests their use in the finite element analysis of plates and shells and also in computer-aided geometric design. In particular, they could be used for the practical implementation of the method proposed by Williams[4] for the production of smooth surfaces.

REFERENCES

1. G. Farin, *Curves and Surfaces for Computer Aided Geometric Design*, Academic Press, London, 1988.
2. O. C. Zienkiewicz, *The Finite Element Method in Engineering Science*, McGraw-Hill, Maidenhead, U.K., 1971.
3. A. S. Day, "An introduction to dynamic relaxation", *The Engineer*, January 1965.
4. C. J. K. Williams, "Use of structural analogy in generation of smooth surfaces for engineering purposes", *Computer-Aided Design* **19**(6), 310–322 (1987).